Journal of Earth Sciences and Geotechnical Engineering, vol. 4, no. 4, 2014, 17-34
ISSN: 1792-9040 (print), 1792-9660 (online)
Scienpress Ltd, 2014

Modelling Approaches Considering Impacts of Water-level Fluctuations on Slope Stability

Jens M. A. Johansson[1] and Tommy Edeskär[2]

Abstract

Waterfront slopes are affected by water-level fluctuations originating from as well natural sources (e.g. tides and wind waves), as non-natural sources such as watercourse regulation involving daily or hourly recurring water-level fluctuations. Potentially instable slopes in populated areas means risks for as well property as human lives. In this study, three different approaches used for hydro-mechanical coupling in FEM-modelling of slope stability, have been evaluated. A fictive slope consisting of a till-like soil material has been modeled to be exposed to a series of water-level fluctuation cycles (WLFC's). Modelling based on assuming fully saturated conditions, and with computations of flow and deformations separately run, has been put against two approaches being more sophisticated, with unsaturated-soil behavior considered and with computations of pore-pressures and deformations simultaneously run. Development of stability, vertical displacements, pore pressures, flow, and model-parameter influence, has been investigated for an increased number of WLFC's. It was found that more advanced approaches did allow for capturing larger variations of flow and pore pressures. Classical modelling resulted in smaller vertical displacements, and smoother development of pore-pressure and flow. Flow patterns, changes of soil density (linked to volume changes governed by suction fluctuations), and changes of hydraulic conductivity, are all factors governing as well water-transport (e.g. efficiency of dissipation of excess pore pressures) as soil-material transport (i.e. susceptibility to internal erosion to be initiated and/or continued). Therefore, the results shown underline potential strengths of sophisticated modelling. Parameter influence was shown to change during water-level cycling.

Keywords: Water-level fluctuations, slope stability, unsaturated soil, FEM

[1] Dept. of Civil, Environmental and Natural Resources Engineering, Luleå University of Technology, Luleå, Sweden.
[2] Dept. of Civil, Environmental and Natural Resources Engineering, Luleå University of Technology, Luleå, Sweden.

1 Introduction

When it comes to recurring water-level fluctuations in watercourses and reservoirs, effects of hydrological changes on slope stability are often overlooked. There is a predominance of studies focused on bioenvironmental issues[1].The activity of watercourse regulation for water storage, enabling irrigation, freshwater provision, and hydropower production, often means occurrence of water-level fluctuations (e.g. [2–4]). The growing use of non-regulated energy sources (e.g. wind and solar) [5, 2, 6, 7]—bringing significant emphasis put on wind-power development and exploitation—entails a need of energy balancing by water storage in reservoirs. According to [8], this will necessarily require that flow magnitudes and water level heights, to a greater extent than until present, will vary in the future. It is highly expected to get increased variations of the reservoir water levels; hour to hour, day to day and/or seasonally[9,2, 4].

The process of rapid draw down is described and investigated by many authors e.g. [10–13]. Also water-level rise might cause problems. In studies concerning the Three Gorges Dam site (e.g. [14]), slope stability reductions registered during periods of water-level rise, have been reported. Rise of water levels has been shown to cause stress redistributions due to external loading, wetting induced loss of negative pore pressures, and seepage effects. Subsequently, these changes have been shown to potentially cause loss of shear strength, soil structure collapse, and development of settlements and/or slope failure[15]. It has been emphasized that a delayed change of pore water pressure inside a slope—relative to the external water level—may result in significant movements of water within the slope; creating seepage forces being adversely affecting the stability[15].

Despite well-known limitations of limit-equilibrium methods (LEM) (e.g.[11, 16]), these are well established and widely used. For capturing important relations between pore pressure, soil strength, and soil-deformation development, the use of finite-element methods (FEM) have been more and more spread. Long-term perspectives are important for consideration of altering hydraulic gradients, stress-strain changes, and development of influenced waterfront zones. Still, reliable relationships between soil deformation, pore-pressure development, and unsteady water-flow conditions are often deliberately overlooked or incidentally missed[1]. Though, improved accessibility of high computer capacity allows for more and more advanced analyses to be performed. In addition, optimized designs and constructions are increasingly demanded and less conservative design approaches are therefore often desired. This is not at least linked to economic and environmental aspects. One non-conservative view in slope-stability analysis regards consideration of negative pore pressures in unsaturated soils. Taking into account negative pore pressures is generally associated with counting on extra contributions to the shear strength of the soil, resulting in extra slope stability. The well-known and widely used Terzaghi´s equation of effective-stress ($\sigma' = \sigma - u$)is simply based upon the difference between the total stress, σ and the pore pressure, u. The equation implies that there are only two possible soil conditions; (1) presence of pore pressure coming from fully water filled pores, and (2) no pore pressure. The validity of this expression is widely accepted in saturated soil mechanics, but has since a long time been found to not be applicable for partly saturated conditions, e.g. [17]. The possibility to control the mechanical response of unsaturated soils by considering two stress-state variables—(1) net stress, i.e. the difference between the total stress and the pore-air pressure, and (2) suction, i.e. the difference between the pore-air pressure and the pore-water

pressure—was firstly demonstrated by [18]. Though, the earliest effective-stress equation for consideration of a varying degree of saturation and suction was presented by Bishop in the end of the 1950th. For description of the amount of water being present in unsaturated soils, soil-water characteristic curves (SWCC) are important. The degree of saturation, S_r (among other alternatively use quantities) appears to most closely control the behavior of unsaturated soil [19]. For proper consideration of the behavior of unsaturated soils, fully coupled hydro-mechanical computations are needed (e.g. [20–22]).

Among studies with hydro-mechanical approaches applied, many are addressing sediment-loading problems; sources, changed river shapes caused by sedimentation etc.(e.g. [23–25]). Consequently, the slope-stability part is ofteneither absent or considered by using LEM-approaches (e.g. [26–28]). There are a few studies addressing effects of large-scale reservoir water-level fluctuations on slope stability; e.g. [29] where saturated-unsaturated seepage analysis was combined with LEM-stability analysis, and [30] where evaluation of the approach of analyzing stability using critical slip fields. The complexity of how factors such as drawdown rate, permeability, and slope height actually do influence the stability of a slope subjected to drawdown, was discussed in [20].

In [31] it was emphasized the misconception concerning that analysis approaches considering principles of unsaturated soil mechanics are always less conservative than are classical ones. It was stated that the overall subject is at its early stage, that there are numerous areas in which practical application of the principles of unsaturated soil mechanics are central, and that as well experimental as theoretical advances are expected.

The present study is aimed to evaluate results from three approaches of hydro-mechanical coupling in FEM-modelling of slope stability; (1) *semi-coupled modelling*, (2) *fully coupled modelling*, and (3) *fully coupled modelling, but with negative pore pressures neglected in stability computations.* In (1) flow computations were run prior to those of deformations, and Terzaghi's effective-stress definition was used. In (2) pore-pressure development and deformations were simultaneously computed, utilizing Bishop's effective-stress definition, considering also the behavior of unsaturated soils. Approach (3) is similar to (2), but with suction effects in stability computation neglected. A fictive waterfront bank slope consisting of a well-graded postglacial till, typical for Swedish conditions, was modeled to be subjected to a series of water-level-fluctuation cycles (WLFC's). Development of stability (in terms of factors of safety, FOS), vertical displacements, pore pressures, flow, and model-parameter influence, was investigated for an increased number of WLFC's. The modelling was performed by use of the software PLAXIS 2D 2012 [32], allowing for consideration of transient flow and performance of coupled hydro-mechanical computations. Moreover, parameter-influence analysis was performed with respect to FOS's calculated using the *strength reduction technique*; i.e. the parameter-influence development with an increased number of WLFC's was investigated.

2 Methodology

2.1 Model Design and Preparations

2.1.1 Geometry, materials, and definition of changes

The model geometry was defined aimed to represent one half of a watercourse cross section. The slope height was set to 30 m, and the slope inclination to 1:2 (26.6°) (**Error! Reference source not found.**); both measures considered to be representative for a watercourse slope consisting of a well-graded till, typical for Swedish conditions (properties presented in Table 1). 15-noded triangular elements were used.

The vertical model boundaries were set to be horizontally fixed and free to move vertically, whereas the bottom boundary was completely fixed. The left vertical boundary was assumed to have properties of a symmetry line, and the model bottom to represent a material being dense and stiff relative to the soil above. Therefore, as well the left vertical hydraulic boundary as the horizontal bottom, were defined as closed (impermeable). The right vertical boundary was defined to be assigned pore pressures by the head, simulating allowed in/out flow. Data-collection points were placed where interesting changes would be expected; at the crest, down along the slope surface, and along a vertical line below the crest.

The initial water-level position was set to +22.0 m (with the level of the watercourse bottom at ± 0 m), the level-change magnitude to 5.0 m (linearly lowered and raised), and the rate to 1.0 m/day. In [33] situations with daily magnitudes of water-level variations in pumped-storage hydropower (PSH) in the order of 10 m were discussed, and in [20] a rate of 1 m/day was used in rapid drawdown analysis. Since this study is comparative, the rate used was chosen in order to create a stability reduction at drawdown, avoid failure, and still be within a relevant and representative range. The water-level changes were run continuously; i.e. without allowing pore pressures to even out.

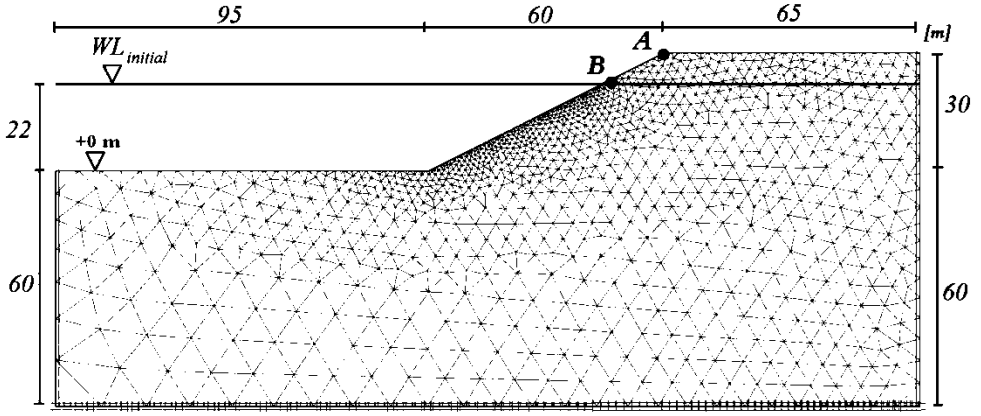

Figure 1: Model geometry. Dimensions, initial water level (WLinitial), and the pre-defined data-collection points—one at the crest (A) and one at the level +22 m (B)—are shown in the figure.

Table 1: Model input data used.

		Unit	*Value*	*Comments*
General				
Drainage type	-	-	Draine	
Unsaturated weight	γ_{unsat}	*kN/m*	19.00	Typical value
Saturated weight	γ_{sat}	*kN/m*	21.00	Typical value
Soil description				
Young´s modulus	E	*kN/m*	40 000	[2]
Poisson´s ratio	ν	-	0.30	[2]
Cohesion	c	*kN/m*	8	Low, non-zero
Friction angle	ϕ	°	36	Typical value
Dilatancy angle	ψ	°	3	Meeting the recommendation $\psi \leq \phi -$
Hydraulic				
Model				van Genuchten
Data set	-	-	-	Defined in order to be representative [1]
Permeability, x	k_x	*m/da*	0.05	Found to be representative (e.g. [34])
Permeability, y	k_y	*m/da*	0.05	Found to be representative (e.g. [34])
Saturated degr. of	S_{sat}	-	1.0	
Residual degr. of sat.	S_{res}	-	0.026	[1]
g_n	-	-	1.169	Parameter linked to water extraction [1]
g_a	-	-	2.490	Parameter linked to air entry [1]
g_l	-	-	0	Parameter linked to pore connectivity [1]

[1]The data set was manually defined by using the parameters listed. The values of the parameters $\boldsymbol{S_{sat}}$, $\boldsymbol{S_{res}}$, $\boldsymbol{g_n}$, $\boldsymbol{g_a}$, and $\boldsymbol{g_l}$ were chosen based on examples in [22], comments in [35], and the pre-defined data set *Hypres* available in PLAXIS 2D 2012 [36].

[2]Within ranges presented in [37]; Young´s modulus for a loose glacial till (10-150 MPa), and for a medium/compact sand (30-50 MPa), at ν=0,30-0,35.

NOTE: Since the result evaluation is comparative, the values of the parameters chosen are not critical.

2.2 Modelling Strategy

2.2.1 Approaches evaluated

Approach 1 (A1): The computations were performed using Terzaghi's definition of stress, i.e. $[\sigma = \sigma' + u]$, where σ is the normal stress, σ' is the effective normal stress, and u is the pore pressure consisting of steady-state pore pressure (from the phreatic level or groundwater flow computations) and excess pore pressure (coming from undrained behavior or consolidation; i.e. temporal pore-pressure changes governed by the WLF's and captured by consideration of transient water flow). In this semi-coupled approach, flow computations were run prior to the deformation computations. Pore pressures from the flow computations were, for each time step, used in the deformation computation for the corresponding time step. The consolidation computations were based on excess pore pressures.

Approach 2 (A2): For the fully coupled approach Bishop's effective-stress equation was used. The consolidation computations were based on the Biot's theory of consolidation [38]; i.e. using total pore pressures with no distinction made between steady state and excess pore pressures.
Approach 3 (A3): Computations run like in A2, but with stability computations run without consideration of negative pore pressures.

2.2.2 Behavior of unsaturated soil

For the fully coupled approaches (A2 and A3), Bishop's effective-stress equation was used, allowing for capturing the unsaturated soil behavior:

$$\sigma' = \sigma - u_a + \chi(u_a - u_w) \quad (1)$$

where u_a is the pore-air pressure, u_w the pore-water pressure, and χ the experimentally determined matric-suction coefficient being related to the degree of saturation, S_r. The experimental evidences of χ are sparse [22], and the role of the parameter has been generally questioned [19]. In PLAXIS 2D 2012 the matric-suction coefficient is substituted with the effective degree of saturation, S_e, defined as:

$$S_e = (S_r - S_{r,min})/(S_{r,max} - S_{r,min}) \quad (2)$$

whereS_r is the degree of saturation and the indices max and min denote maximum and minimum values. Moreover, in this study the air-pore pressure is assumed to be negligibly low, whereupon the effective stress is simply expressed as:

$$\sigma' = \sigma - S_e u_w \quad (3)$$

The effective degree of saturation is used also for definition of actual soil unit weight, γ:

$$\gamma = (1 - S_e)\gamma_{unsat} + S_e\gamma_{sat} \quad (4)$$

where the indices denote unsaturated and saturated conditions.

2.2.3 Models used

The constitutive behavior of the soil was described by Mohr-Coulomb's elastic-perfectly plastic model. This model was chosen for three reasons; (1) it is well-established and widely used by engineers, (2) as soon as the stability analysis is started (performed using the strength reduction technique), any model defined with the same strength parameters would behave like the Mohr-Coulomb model (i.e. stress dependent stiffness is excluded), (3) the study is comparative whereupon differences between the modelling approaches evaluated are focused rather than the accuracy of the soil description. For other permissions/claims, models like e.g. the Hardening soil model [32] (allowing for description of more realistic elastic-plastic behaviors), or the Basic Barcelona Model [39] (specifically developed for description of the stress-strain behavior in unsaturated soils), could have been used. The soil was defined by the variables listed in Table 1. The elastic behavior is described by the parameters Young´s modulus, E and Poisson´s ratio, ν. The full three-dimensional yield criterion consists of six yield functions; two functions in each plane of stress pairs. Each yield function depends on one stress pair (one combination of

the principal effective stresses), the friction angle, ϕ' and the cohesion, c'. These are defining the ultimate state up to which the strains are elastic; for stress conditions entailing that the yield function is reached, the strain response becomes perfectly plastic. For these conditions the strain magnitudes are determined using flow rules based on plastic potential functions. These are—similar to the yield functions—depending on the stress state, but are consisting of three plastic parameters; in addition to the friction angle, ϕ and the cohesion, c, also the dilatancy angle, ψ. This parameter is used for description of additional resistance against shearing, originating from dilatant behavior.

For description of hydraulic behavior in the soil, van Genuchten's model [40] was used. The important role of the hydraulic model is to properly define the degree of saturation, S_r as a function of suction pore-pressure head, h_p. This relation, often presented in soil-water characteristic curves (SWCC), is expressed:

$$S_r(h_p) = S_{res} + (S_{sat} - S_{res})\left[1 + (g_a|h_p|)^{g_n}\right]^{\frac{1-g_n}{g_n}} \tag{5}$$

where S_{res} is the residual degree of saturation, S_{sat} is the saturated degree of saturation, g_a is an empirical parameter describing air entry, and g_n is an empirical parameter related to the water extraction from the soil. The relative permeability, $k_{rel}(S_r)$ is expressed as:

$$k_{rel}(S_r) = {S_e}^{g_l}\left[1 - \left(1 - {S_e}^{\frac{g_n}{g_n-1}}\right)^{\frac{g_n-1}{g_n}}\right]^2 \tag{6}$$

where g_l is an empirical parameter. The relative permeability is in the flow computation reducing the permeability k according to $(k_{rel} = k/k^{sat})$ where k^{sat} is the saturated permeability.

Factor of safety

The strength reduction (or phi/c-reduction) technique is based on FOS's defined as the ratio between the available shear strength and the shear stress at failure. In PLAXIS 2D 2012 this is mathematically handled by expressing ratios of the strength parameters:

$$\Sigma M_{sf} = \frac{c}{c_{reduced}} = \frac{\tan\phi}{\tan\phi_{reduced}} \tag{7}$$

where M_{sf} is a controlling multiplier representing the safety factor; c is the cohesion; ϕ is the friction angle; and the index reduced indicates values being successively decreased until failure occurs. For indication of global instability of soil slopes, the non-convergence of solutions is often used. This is indicated by the condition when a stress state at which the failure criterion and the global equilibrium can be simultaneously satisfied, is not found [10].

Parameter-sensitivity analysis

The parameter influence was investigated with respect to changed FOS. For each parameter, a maximum and a minimum value were defined spanning a representative interval within which the reference value for each parameter (presented in Table 1) was

located. The theories used are based on the ratio of the percentage change of the result, and the percentage change of input (creating the output change); explained in e.g. [41]. The sensitivity ratio η_{SR}[42] is expressed as:

$$\eta_{SR} = \left(\frac{F(x_{U,L}) - F(x)}{F(x)}\right) \Big/ \left(\frac{x_{U,L} - x}{x}\right) \tag{8}$$

where the output values are functions, F of the input values, x for which no index represents the reference input values and the index U,L represents the changed ones; upper/lower. In order to increase the robustness [32] of the analysis, the sensitivity ratio was weighted by a normalized variability measure. This was done using a sensitivity score, η_{SS}, defined as the ratio of the range itself and the variable mean value [42]:

$$\eta_{SS} = \eta_{SR} \cdot \left(\frac{\max x - \min x}{x}\right) \tag{9}$$

where$\max x$ and $\min x$ define the range limits, and x is the mean (reference) value. The total sensitivity was then calculated as:

$$\eta_{SS,total} = \left(\frac{{\eta_{SS}}^{U} + {\eta_{SS}}^{L}}{\sum \eta_{SS}\,(\text{all parameters})}\right) \tag{10}$$

where ${\eta_{SS}}^{U}$ and ${\eta_{SS}}^{L}$ are the sensitivity scores connected to the upper and lower parameter value, respectively, and $\sum \eta_{SS}$ is the sum the sensitivity scores of all parameter combinations. Five model parameters were considered in the analysis; the variation boundaries are presented in Table 2. For each parameter, one computation was run for each range boundary, keeping the other parameters fixed. This was giving the sensitivity ratios (eq. 8) and the sensitivity scores (eq. 9). The total scores (eq. 10) were then plotted.

Table 2: Soil parameters used in the sensitivity analysis (Min and Max), and the reference values.

E (MPa)			*ν (-)*			*ϕ (°)*			*c (kPa)*			*ψ (°)*		
Min	Ref	Max	Min	Ref	Max	Min	Ref	Max	Min	Ref	Max	Min	Ref	Max
20	**40**	60	0.25	**0.30**	0.35	33	**36**	39	1	**8**	15	0	**3**	6

2.3 Computations

The computations were performed in PLAXIS 2D 2012 [32]. This FEM-code was used since it is well-established and providing what was needed. The bank was assumed to be infinite in the direction perpendicular to the model plane; i.e. 2D plain-strain conditions were assumed. A1 was performed in Classical calculation mode whereas A2 and A3 were run in Advanced mode. The initial stress situation was determined by a Gravity loading phase; providing initial stresses generated based on the volumetric weight of the soil (this since the non-horizontal upper model boundary means that the K0-procedure is not suitable). Then a plastic nil-step was run, solving existing out-of-balance forces and

restoring stress equilibrium. The WLFC's were defined in separate calculation steps; one drawdown-rise cycle in each. Each WLFC was followed by a FOS-computation. In A3, each FOS-computation was preceded by a plastic nil-step; this to restore the stress equilibrium in order to omit consideration of negative pore pressures. Sensitivity analyses were carried out for the three approaches.

3 Results and Comments

3.1 Model Design and Preparations

In Figure the failure plots from A1 are shown; conditions at the initial stage (Init.), after one rapid drawdown (RDD), and after one WLFC (1). Fully developed failure surfaces were found for all WLFC's in all of the approaches.

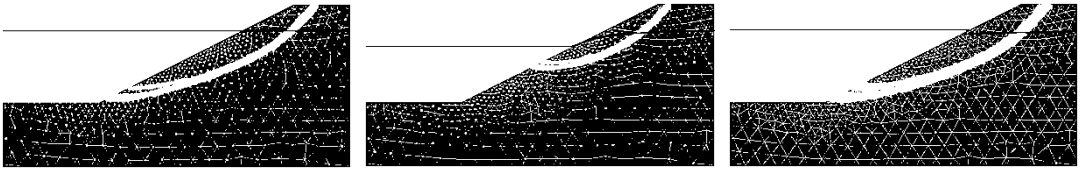

Figure 2: Failure surfaces for the initial condition, after one rapid drawdown, and after one WLFC, for approach A1.

The changed failure-surface geometry—moved upward at drawdown—shows the supporting effect of the external water level. Since the slope was stable also after the drawdown, the reference parameter values and geometry used was found to be suitable for further analysis. The FOS-development is presented in Figure Error**! No text of specified style in document.**.

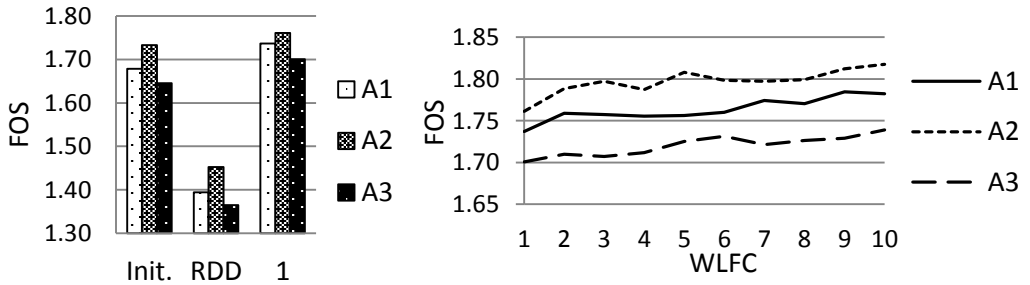

Figure **Error! No text of specified style in document.**: FOS-values for initial conditions (Init.), after one rapid drawdown (RDD), and after one WLFC (1) (picture to the left); and development by additional WLFC's (picture to the right).

For all approaches—with the initial conditions as references—the FOS-values were significantly decreasing due to the rapid drawdown (about 17% for A1, and 16% for A2 and A3), slightly increasing due to the first WLFC (3% for A1 and 2% for A2 and A3), and ending up exhibiting further increased values after 10 WLFC's (a total increase of 6 % for A1, and 5% for A2 and A3). The results show that the stability growth continues during the entire period studied.

Lower FOS-values were obtained using the approach assuming saturated conditions below the water-level, dry conditions above, and taking into account neither pore-pressure changes due to deformations, nor suction (A1), than using fully coupled flow-deformation computations, considering also suction forces (A2). This is reasonably explained by the consideration taken to the contribution of suction forces to the stability. The lowest FOS-values were obtained in A3; i.e. fully coupled flow-deformation computations, but with the negative pore pressures not considered in the stability analysis. These FOS-values were found to be even lower than those obtained in A1; this although suction was neglected also in A1.

3.2 Deformations, Pore Pressures and Flow

In **Error! Reference source not found.**, vertical deformations developed at the crest (point A, see **Error! Reference source not found.**) are presented. The values were registered in the middle of each WLFC, i.e. at the end of each drawdown.

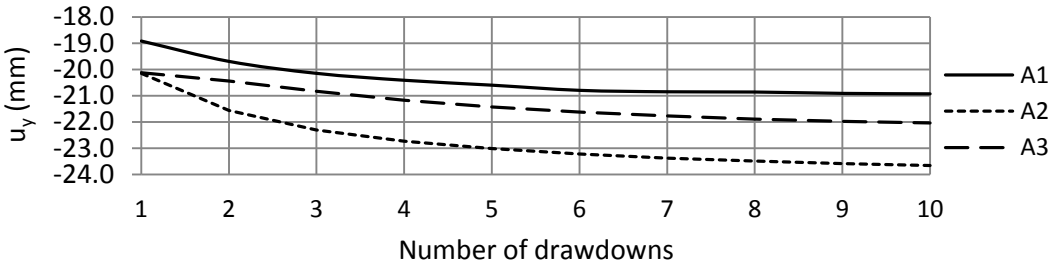

Figure 4: Vertical deformations at the crest; readings from the end of each drawdown. The reference level before the first drawdown is 0 mm.

The overall pattern is the same in all approaches; additional vertical deformations are developed with an increased number of drawdowns. The rate is decreasing although a definitive asymptotical pattern cannot be seen. Utilization of A1 seems to give less deformations developed compared to both A2 and A3. This was found to be true at all depths vertically below point A (see **Error! Reference source not found.**).

The development of the active pore pressure, p_{active} (consisting of contributions from as well steady state as excess pore pressure) measured in A2, is shown in **Error! Reference source not found.**. The developments were registered in two different points; one located at the crest (point A in **Error! Reference source not found.**), and one at the initial groundwater level (point B in **Error! Reference source not found.**).

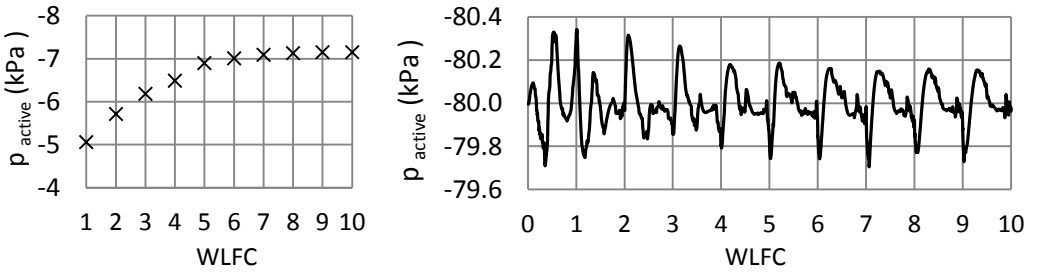

Figure 5: Pore-pressure development from A2, registered in point B (picture to the left),

and in point A (picture to the right).

For point B only peak-values are presented, registered at the end of each WLFC. The development in between was found to be smooth/non-fluctuating. The development of the peak values shows how the active pore pressure—at the end of each WLFC—slowly becomes more and more negative; an increase exhibiting a higher rate between 1 and 5 WLFC's than for further cycling, seeming to be asymptotically fading out. The increase of the negative pore pressure indicates that the groundwater table is dropping for each cycle. To the right, suction effects above the water level is clearly seen. Also in this plot there is a fading out pattern.

In **Error! Reference source not found.** a typical picture of the flow region—the area where the external water level and the slope surface intersect—is shown. The external water level is back to the level +22, immediately after one WLFC has been run, whereas the groundwater table is lagging behind.

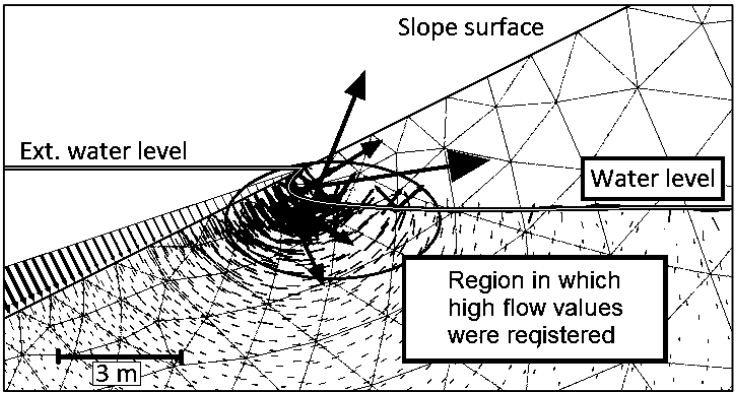

Figure 6: A sample picture of the area where the external water level and the slope intersect, showing the hydraulic conditions prevailing immediately after the first WLFC run in A1. The external water level is located at +22 m whereas the groundwater table within the slope is lower. The flow directions are presented by arrows.

In **Error! Reference source not found.**, **Error! Reference source not found.** and **Error! Reference source not found.** flow conditions immediately after each WLFCare plotted. Since the readings were taken at the end of each cycle, the external water level and the groundwater table are almost coinciding, meaning small absolute magnitudes of the flow values registered. The flow condition for each stageis presented as the deviation from the average valueof the 10 cycles. Maximum total flow,$|q_{max}|$ and horizontal flow directed inwards (in to the slope), $q_{x,right}$is presentedin**Error! Reference source not found.**, whereas maximum vertical flow (upward directed, $q_{y,up}$, and downward directed, $q_{y,down}$) is shown in **Error! Reference source not found.**. All of the maximum and minimum valuesare originating from the region being markedin **Error! Reference source not found.**, except the $q_{x,,right}$–values. The latter ones are registered just below the groundwater table, approximately 10 m right (inwards) from the slope surface.

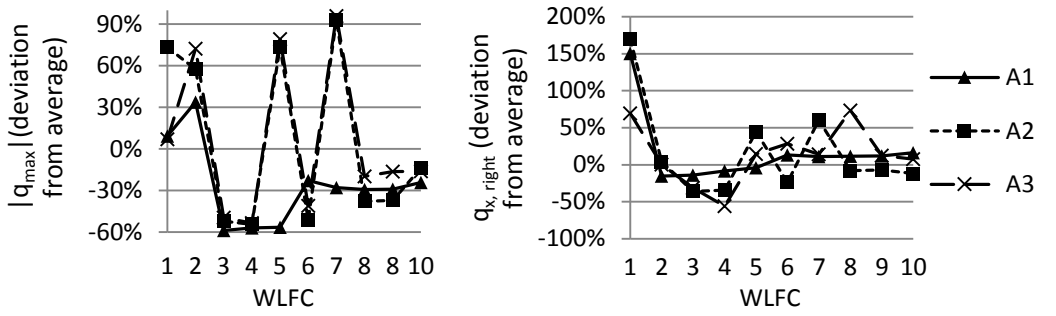

Figure 7: Maximum total flow in the slope; average ~0.1 m/day (picture to the left), and rightward directed horizontal flow; average ~ 0.08 m/day (picture to the right).

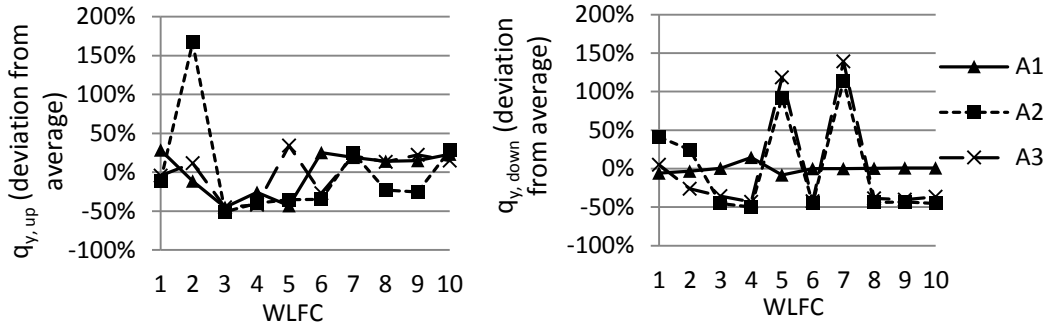

Figure 8: Maximum upward directed flow (picture to the left), and downward directed flow (picture to the right); both averages ~0.05 m/day.

The flow magnitudes were found to change from one stage to another; i.e. by increased number of cycles. Larger flow changes were captured using the fully coupled flow-deformation computations (A2 and A3), compared to in A1. The difference is particularly pronounced for the rightward directed horizontal flow, $q_{x,right}$ and the downward directed vertical flow, $q_{y,down}$. Regarding $|q_{max}|$ and $q_{y,down}$,the results from A2 and A3 are to a large extent coinciding. In **Error! Reference source not found.**, development of vertical flow, $q_y$and horizontal flow, q_x—extracted from the same stress point in all approaches—are shown. The point is located approximately 1 m below the initial water level, 1 m to the right from the slope surface.

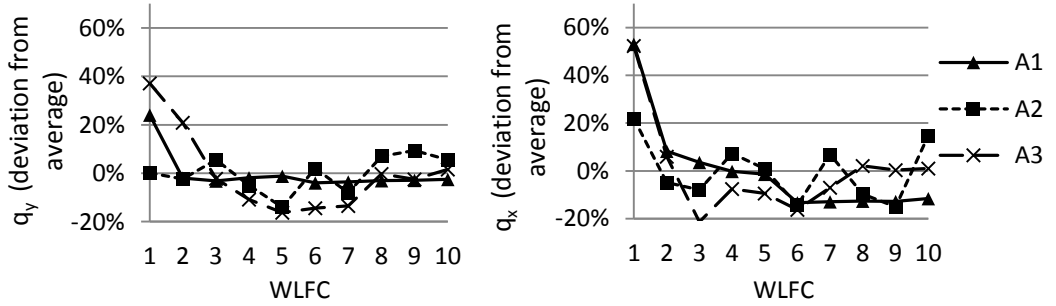

Figure 9: Vertical flow (picture to the left), and horizontal flow (picture to the right); both averages ~0.05 m/day.

Again, larger flow deviations were captured in A2 and A3, compared to in A1.

3.3 Parameter Influence

The sensitivity analysis did provide parameter-influence values; total sensitivity ($\eta_{SS,total}$). In **Error! Reference source not found.** the total sensitivity values (on the y-axis) for each of the five parameters at initial state (Init.), after one rapid drawdown (RDD), and after one WLFC (1), are shown.

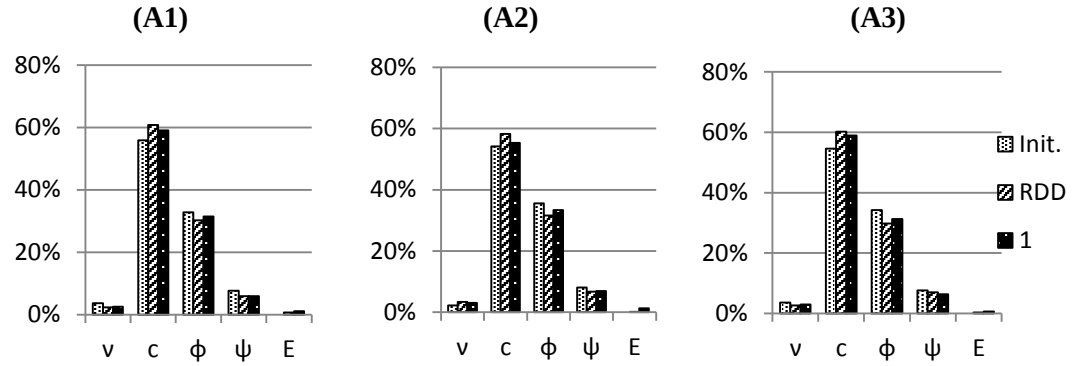

Figure 10: The influence (in terms of sensitivity) of each parameter, with respect to safety (in terms of FOS).

The stiffness parameters are influencing the stability significantly less than are the strength parameters. The cohesion, c exhibits the highest influence in all approaches; followed by the influence of the friction angle, ϕ and the dilatancy angle, ψ. The influence of as well Poisson's ratio, ν as of Young's modulus, E is slightly increasing during further cycling; though remaining below 3% and 2%, respectively. Therefore, the stiffness parameters are excluded from the presentation of further sensitivity development, presented in **Error! Reference source not found.**.

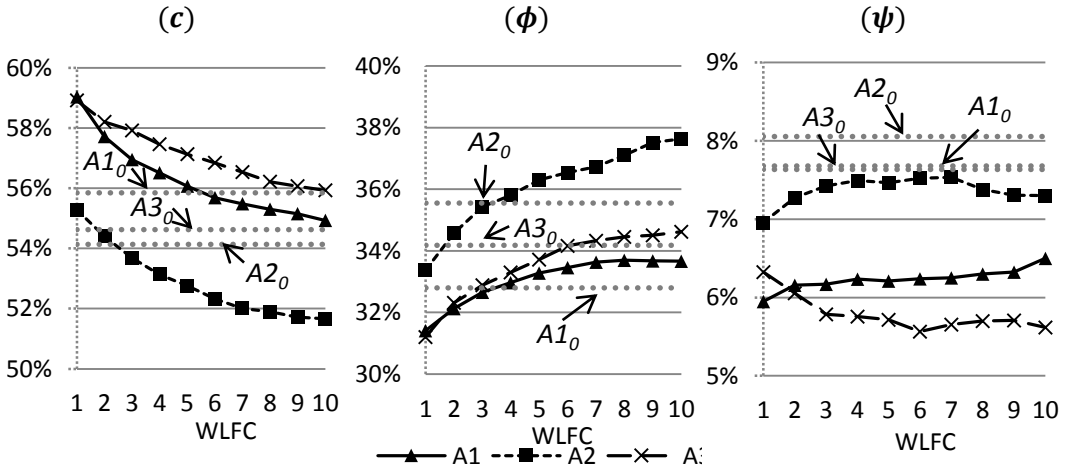

Figure 11: Sensitivity development. The dotted lines are showing the initial values for

each modelling approach ($A1_0$,$A2_0$, and $A3_0$).

It is clear that the sensitivity values are depending on the stage at which the safety is evaluated, i.e. on the numbers of WLFC's run. For cohesion, c the qualitative trend is the same in all cases; maximum influence at drawdown and then declining with increased number of WLFC's. In A1 the sensitivity of cohesion gets lower than the initial value after 5 WLFC's; in A2 this occurs at 2 WLFC's, and in A3 the initial value is not reached during the 10 cycles. For the friction angle, ϕ the pattern is opposite; minimum values at drawdown and then increasing. For this parameter, the initial values are exceeded in all approaches; in A1 and A2 at 3 WLFC's, and in A3 at 6 WLFC's. The total change (decrease) of the influence of cohesion (during 10 cycles) seems to be similar in all approaches, whereas the increase of the friction-angle influence in A2 seems to be fading out slower than in A1 and A3. When it comes to the dilatancy angle, ψ the patterns are more scattered. In all cases the sensitivity values are decreased after the first drawdown, whilst the further development is almost constant. Though, the absolute magnitudes (and the variations) of the dilatancy-angle influence are very small, and further conclusions are not reasonably drawn.

4 Discussion

Despite the fact that the absolute magnitudes of differences identified in this study were small—FOS-values, pore pressures, flows etc.—these do nonetheless demonstrate important dissimilarities concerning the ability to capture/simulate real soil-water interactions and changes. The results of FOS-development show that the stability growth continues during the entire period studied; though not smoothly. The stability increase is to assign to the fact that the groundwater table is dropping (remained at a lower level) for each WLFC; this was also confirmed by the pore-pressure developments discussed. Lower FOS-values were obtained using the classical approach, A1 than those obtained using approach A2. This could be reasonably explained by the consideration taken to the contribution of suction forces to the stability in A2. The fact that the lowest FOS's were obtained by using A3, would suggests that this approach is most conservative in this study, in the sense of not overestimating the stability. This is unexpected since suction was not considered at all in A1, whereas suction was considered throughout the entire cycle in A3, until the FOS-computation was run. Anyhow, whether the unexpected result is connected to the nil-steps computed in A3 done in order to neglected suction, or to unrealistic computation of the soil weight above the water level, the FOS result of A3 is to be treated with caution.

Use of A1 resulted in smaller vertical crest deformations compared to the other approaches. This suggests that the two-way interaction between pore pressure changes and deformation development in the fully coupled computations (A2 and A3), could capture conditions that bring larger deformations. This means a potential underestimation in A1. Moreover, the flow developments registered in A2 and A3 were significantly more fluctuating than those in A1; as well horizontally as vertically. The difference was seen to be particularly pronounced for the rightward directed horizontal flow, and the downward directed vertical flow. In agreement with what was stated in [31], also the outcomes from the present study show that there seems to be situations where computations taking into account unsaturated soil behavior, is not necessarily less conservative than are classical

ones.
The parameter-sensitivity analysis results obtained using A1 seems to be quantitatively more comparable to those obtained using A3 than to those using A2. This suggests that consideration of suction at stability computation (only true in A2), does directly affect the parameter influence on the results. However, major differences were not found. Since the sensitivity was computed with respect to FOS determined by using the strength reduction technique, the low and insignificantly changing sensitivity values of the stiffness parameters were expected. The non-constant sensitivity values of the dilatancyangle, might indicate that the occurrences of plastic strains are somewhat different in the different stages. Though, the influence is significantly lower th an for friction angle and cohesion, and also less changing.
It might be useful to consider parameter influence for evaluation of the accuracy needed for definition of model input data; as well absolute magnitudes, as the development patterns. Moreover, when making up modelling/design strategies, parameter changes (e.g. by time or by external changes taking place), could be valuably included.
The results obtained in this study are reflecting effects occurred under the specified conditions of hydraulic conductivity, rate of water-level change, and slope geometry. Since these factors are unquestionably affect processes taking place within a watercourse slope, it would be reasonable to include variation also of such non-constitutive parameters in further studies.
Since fully coupled flow-soil deformation modelling to a higher degree describes real soil-water interaction, results from semi-coupled approaches (like A1) are probably not optimal for analysis of processes being governed by fluctuating flows, altering hydraulic gradients, unloading/reloading etc. Since hydraulic models do partly rely on empirical soil-specific parameters there are potential uncertainties connected to the level of accuracy of these. Still, this uncertainty is to be related to the extra information possibly obtained at consideration of specific features of unsaturated soils. Flow patterns, changes of denseness, and non-constant values of the hydraulic conductivity, are all factors being valuable for proper modelling. Not at least since such changes in turn are governing as well water-transport (i.e. the efficiency of dissipation of excess pore pressures), as soil-material transport (i.e. susceptibility to internal erosion to be initiated and/or continued).

5 Concluding Remarks

- The soil structure seems to become more stable due to the first WLFC, and the stability growth continues during the entire period studied. This for all approaches.
- Modelling assuming strictly saturated or dry conditions (classical, like in A1) resulted in—restricted to slope stability in terms of safety factors—higher conservatism compared to modelling considering also the behavior of unsaturated soil and fully hydro-mechanical coupling (advanced, like in A2).
- Modelling considering the behavior of unsaturated soil and fully hydro-mechanical coupling, but with suction neglected at stability computation (A3) resulted in lower safety factors even compared to classical modelling (A1). This might be explained by errors due to the saturation-suction relation in the hydraulic model used, or to the nil-step computations run in order to get the negative pore pressure neglected.
- Advanced modelling seems to allow for rapid changes of pore pressures and flow to

be more realistically captured compared to classical modelling. Such changes in turn are governing as well water-transport (i.e. the efficiency of dissipation of excess pore pressures), as soil-material transport (i.e. susceptibility to internal erosion to be initiated and/or continued).

- The influence of the parameters were changing as a result of WLFC's taking place; decreased influence of cohesion, increased influence of the friction angle, scattered patterns of the influence of the dilatancy angle.

5.1 To be further considered

In order to capture effects of water-level variation frequencies, rates, slope geometries etc., on slope stability, investigations should be performed using advanced modelling approaches, and considering real long-term perspectives. Use of a more advanced constitutive soil model (e.g. the Hardening soil model [32]) would potentially reduce inaccuracy coming from e.g. improper description of plastic deformations and stiffness changes. The water-level fluctuation effects would also be investigated using models based on the Basic Barcelona Model [39]. Parameter influence would be preferably considered when evaluating the accuracy needed for modelling-input data, as well as when making up modelling/design strategies. Investigations of processes taking place within slopes being subjected to recurrent WLF's, would desirably be conducted. For instance by laboratory/scale tests combined with modelling.

ACKNOWLEDGEMENTS: The research has been supported by the Swedish Hydropower Centre, SVC; established by the Swedish Energy Agency, Elforsk and SvenskaKraftnät together with Luleå University of Technology, The Royal Institute of Technology, Chalmers University of Technology and Uppsala University. Participatingagencies, companies and industry associations are: Alstom Hydro Sweden, Andritz Hydro, Energimyndigheten, E.ON Vattenkraft Sverige, Falu Energi och Vatten, Fortum Generation, Holmen Energi, Jämtkraft, Jönköping Energi, Karlstads Energi, Mälarenergi, Norconsult, PöyrySwedPower, Skellefteå Kraft, Sollefteåforsens, Statkraft Sverige, SveMin, Svenska Kraftnät, SwecoInfrastructure, SwecoEnerguide, Umeå Energi, Vattenfall Vattenkraft, VG Power, WSP and ÅF.

References

[1] J. M. A. Johansson and T. Edeskär, "Effects of External Water-Level Fluctuations on Slope Stability," *Electron. J. Geotech. Eng.*, **19**, no. K, pp. 2437–2463, 2014.

[2] O. Mill, A. Dahlbäck, S. Wörman, S. Knutsson, F. Johansson, P. Andreasson, J. Yang, U. Lundin, J.-O. Aidanpää, H. Nilsson, M. Cervantes, and S. Glavatskih, "Analysis and Development of Hydro Power Research - Synthesis within Swedish Hydro Power Centre," Stockholm, 2010.

[3] N. Dahlbäck, "Utvecklingsbehov inom reglerkraftsområdet ur ett vattenkraftperspektiv," Stockholm, 2010.

[4] E. Solvang, A. Harby, and Å. Killingtveit, "Increasing balance power capacity in Norwegian hydroelectric power stations," 2012.

[5] M. Whittingham, "Materials challenges facing electrical energy storage," *Mrs Bull.*, **33**(4), pp. 411–419, Jan. 2008.
[6] D. Connolly, "A Review of Energy Storage Technologies - For the integration of fluctuating renewable energy," PhD thesis, University of Limerick., Limerick, Ireland, 2010.
[7] REN21, "Renewables 2013: Global Status Report," 2013.
[8] Svenska Kraftnät, "Storskalig utbyggnad av vindkraft," 2008.
[9] Svenska Energimyndigheten, "Vattenkraften och energisystemet-ER 2008:24," Eskilstuna, Sweden, 2008.
[10] P. A. Lane and D. V. Griffiths, "Assessment of Stability of Slopes under Drawdown Conditions," *J. Geotech. Geoenvironmental Eng.*, **126**(5), pp. 443–450, May 2000.
[11] J. M. Duncan and S. G. Wright, *Soil Strength and Slope Stability*. Hoboken, New Jersey: John Wiley & Sons, Inc., 2005.
[12] H. Yang, H. Rahardjo, and D. Xiao, "Rapid Drawdown of Water Table in Layered Soil Column," in *Geoenvironmental engineering and geotechnics: progress in modeling and applications*, 2010, pp. 202–209.
[13] N. M. Pinyol, E. E. Alonso, J. Corominas, and J. Moya, "Canelles landslide: modelling rapid drawdown and fast potential sliding," *Landslides*, **9**(1), pp. 33–51, May 2011.
[14] R. Cojean and Y. J. Caï, "Analysis and modeling of slope stability in the Three-Gorges Dam reservoir (China) — The case of Huangtupo landslide," *J. Mt. Sci.*, **8**(2), pp. 166–175, Mar. 2011.
[15] G. W. Jia, T. L. T. Zhan, Y. M. Chen, and D. G. Fredlund, "Performance of a large-scale slope model subjected to rising and lowering water levels," *Eng. Geol.*, **106**(1–2), pp. 92–103, May 2009.
[16] J. Krahn, "The 2001 R.M. Hardy Lecture: The limits of limit equilibrium analyses," *Can. Geotech. J.*, **40**(3), pp. 643–660, Jun. 2003.
[17] J. B. Burland and J. E. B. Jennings, "Limitations to the Use of Effective Stresses in Partly Saturated Soils," *Géotechnique*, vol. 12, no. 2, pp. 125–144, Jan. 1962.
[18] D. G. Fredlund and N. Morgenstern, "Stress state variables for unsaturated soils," *J. Geotech. Geoenvironmental Eng.*, **103**(GT5), pp. 447–466, Jul. 1977.
[19] D. G. Fredlund, "Unsaturated Soil Mechanics in Engineering Practice," *J. Geotech. Geoenvironmental Eng.*, **132**(3), pp. 286–321, Mar. 2006.
[20] M. M. Berilgen, "Investigation of stability of slopes under drawdown conditions," *Comput. Geotech.*, **34**(2), pp. 81–91, Mar. 2007.
[21] M. Huang and C.-Q. Jia, "Strength reduction FEM in stability analysis of soil slopes subjected to transient unsaturated seepage," *Comput. Geotech.*, **36**(1–2), pp. 93–101, Jan. 2009.
[22] V. Galavi, "Internal Report - Groundwater flow, fully coupled flow deformation and undrained analyses in PLAXIS 2D and 3D," 2010.
[23] S. E. Darby, M. Rinaldi, and S. Dapporto, "Coupled simulations of fluvial erosion and mass wasting for cohesive river banks," *J. Geophys. Res.*, **112**(F3), p. F03022, Aug. 2007.
[24] G. A. Fox, G. V Wilson, A. Simon, E. J. Langendoen, O. Akay, and J. W. Fuchs, "Measuring streambank erosion due to ground water seepage: correlation to bank pore water pressure, precipitation and stream stage," *Earth Surf. Process. Landforms*, **32**(10), pp. 1558–1573, Sep. 2007.

[25] J. R. Grove, J. Croke, and C. Thompson, "Quantifying different riverbank erosion processes during an extreme flood event," *Earth Surf. Process. Landforms*, **1406**, no. February, p. n/a–n/a, Feb. 2013.
[26] M. Rinaldi and N. Casagli, "Stability of streambanks formed in partially saturated soils and effects of negative pore water pressures: the Sieve River (Italy)," *Geomorphology*, pp. 253–277, 1999.
[27] A. Simon, A. Curini, S. E. Darby, and E. J. Langendoen, "Bank and near-bank processes in an incised channel," *Geomorphology*, **35**(3–4), pp. 193–217, Nov. 2000.
[28] a. Samadi, E. Amiri-Tokaldany, and S. E. Darby, "Identifying the effects of parameter uncertainty on the reliability of riverbank stability modelling," *Geomorphology*, **106**(3–4), pp. 219–230, May 2009.
[29] T. Zhan, W. Zhang, and Y. Chen, "Influence of reservoir level change on slope stability of a silty soil bank," in *The Fourth International Conference on Unsaturated Soils, ASCE, April 2–4*, 2006, pp. 463–472.
[30] Y. Shen, D. Zhu, and H. Yao, "Critical slip field of slope in process of reservoir water level fluctuations," *Rock Soil Mech.*, **31**(S2), pp. 179–183, 2010.
[31] D. Sheng, S. Zhang, and Z. Yu, "Unanswered questions in unsaturated soil mechanics," *Sci. China Technol. Sci.*, **56**(5), pp. 1257–1272, Apr. 2013.
[32] PLAXIS, "PLAXIS 2D 2012." Available at: http://www.plaxis.nl/, Delft, Netherlands., 2012.
[33] L. M. Rognlien, "Pumped storage hydropower development in Øvre Otra, Norway," Norwegian University of Science and Technology, 2012.
[34] J. Lafleur, "Filter testing of broadly graded cohesionless tills," *Can. Geotech. J.*, **21**(4), pp. 634–643, Nov. 1984.
[35] A. I. Gärdenäs, J. Šimůnek, N. Jarvis, and M. T. van Genuchten, "Two-dimensional modelling of preferential water flow and pesticide transport from a tile-drained field," *J. Hydrol.*, **329**(3–4), pp. 647–660, Oct. 2006.
[36] PLAXIS, "PLAXIS 2D 2012," *PLAXIS Material Models Manual 2012*, 2012. [Online]. Available: http://www.plaxis.nl/files/files/2D2012-3-Material-Models.pdf. [Accessed: 15-Mar-2014].
[37] J. Briaud, *Geotechnical Engineering: Unsaturated and Saturated Soils*. John Wiley & Sons, Inc., 2013.
[38] M. A. Biot, "General Theory of Three-Dimensional Consolidation," *J. Appl. Phys.*, **12**(2), p. 155, 1941.
[39] E. E. Alonso, A. Gens, and A. Josa, "A constitutive model for partially saturated soils," *Géotechnique*, **40**(3), pp. 405–430, Jan. 1990.
[40] M. T. van Genuchten, "A Closed-form Equation for Predicting the Hydraulic Conductivity of Unsaturated Soils," *Soil Sci. Soc. Am. J.*, **44**(5), pp. 892–898, 1980.
[41] U.S. EPA, "TRIM, Total Risk Integrated Methodology, TRIM FATE Technical Support Document, Volume I: Description of Module," 1999.
[42] U.S. EPA, "Risk Assessment Guidance for Superfund (RAGS) Volume III - Part A: Process for Conducting Probabilistic Risk Assessment (2001) - Appendix A," 2001.